Journal of Applied Polymer Science

In vivo bioactivity of herbal-drug-incorporated nanofibrous matrixes

Agnes Mary S., V. R. Giri Dev
Department of Textile Technology, Anna University, Chennai 600 025 Tamil Nadu, India
Correspondence to: V. R. Giri Dev (E-mail: vrgiridev@yahoo.com)

ABSTRACT: Aloe-vera-incorporated polycaprolactone nanofibrous matrixes were prepared by an electrospinning method. These developed matrixes were evaluated for their water absorption capacity, water vapor permeability, and contact angle, and, in an *in vivo* animal model, wound-healing ability. The incorporation of the herbal drug made the matrixes hydrophilic with improved water retention and permeability properties. The *in vivo* studies were carried out in a rat model and showed improved results with respect to healing. Thus, this study confirmed that the developed matrixes could be used for wound-healing applications. © 2015 Wiley Periodicals, Inc. J. Appl. Polym. Sci. **2015**, *132*, 42178.

KEYWORDS: biocompatibility; biodegradable; bioengineering; biomaterials; biomedical applications

Received 30 June 2014; accepted 25 February 2015
DOI: 10.1002/app.42178

INTRODUCTION

Both acute and chronic wounds require attention and treatment. The clinical challenges depend on the severity of the wounds, and this includes wounds from surgical operations that exhibit postoperative complications and those produced as a result of diabetes, skin tumors, accidents, and other external causes. The current estimation of chronic wound occurrence in Indian epidemiology is reported to be 4.5 per 1000 people in the case of acute wounds and 10.5 per 1000 people in the case of chronic wounds.[1] Although it has been estimated worldwide that more than 6 million people suffer from chronic wounds, chronic wounds fail to reconstitute faster as they require a prolonged time to heal completely and, as such, seriously affect the patient's quality of life.[2] The selection of wound dressings for chronic wounds is a complex matter and depends on a number of factors.

The general requirement for an ideal wound dressing is that it should maintain a moist environment at the wound site, absorb excess exudates of wound, be nonadherent in nature, be easy to handle, be nontoxic and nonallergenic, provide a modest debridement action, provide mechanical stability, and provide protection against microbial invasion and contamination.[3] Wound-dressing materials are broadly classified on the basis of the nature of the dressing and the target of action. Bioactive dressings are those that are produced from a variety of biopolymers; these include collagen, gelatin, hyaluronic acid, and chitosan and also those with certain active ingredients, such as plant extracts, antibiotics, and antimicrobials to fight against infections and contaminations.[4]

The incorporation of bioactive agents is a fascinating field of research and development both for curing wounds and providing other healthcare benefits.[5] Even though this traditional medicinal treatment paves the way for the safe and inexpensive treatment of wounds, it has not gained much attention among the research fraternity. Medicinal plant extracts as pastes and ointments are available in the market to promote wound healing and repair injured tissue in a natural way. Even crude extracts of these valuable plants are known to have secondary metabolites, growth factors, and other bioactive compounds that are helpful in healing chronic and acute wounds.[6]

Among these plants, aloe vera (AV) is one of the oldest medicinal plants used by mankind for its healing properties.[7] AV has a complex chemical composition of active ingredients and is mainly composed of soluble sugars, anthraquinones, polysaccharides, amino acids, vitamins, and proteins, all of which could aid in wound healing.[8] Moreover, the plant juice of AV possesses antrakinons with antimicrobial, antiviral, antifungal, and anti-inflammatory properties, and the saponins with antiseptic properties are effective in preventing wound and burn infections. Certain studies on AV extract have revealed that it can heal diabetic ulcers and stimulate collagen synthesis to stimulate the proper healing of wounds.[9] The polysaccharides present in AV are known to enhance the macrophage activity in the wound site and provide improved activity of healing.[10] Generally, these bioactive compounds are prepared as pastes and ointments and applied topically to wounds. Recently, the use of electrospun nanofibrous nonwoven membranes as wound-dressing materials has gained a significant momentum in the field of biomedical tissue engineering.[11] However, only limited attempts have been

made to couple herbal bioactive compounds in nanofibrous matrixes. Recently, studies of herbal-extract-incorporated nanofibrous membranes have suggested that the incorporation of herbal extracts has influenced the wetting behavior of the matrixes and, in turn, supported the fibroblast cells to adhere, proliferate, and regenerate. This, in turn, has facilitated rapid wound healing.[12–18] Moreover, the electrospun dressing materials resemble the extracellular matrix. These matrixes also act as a reservoir for these bioactive agents for prolonged release at the wound bed.[19,20]

Polycaprolactone (PCL) a biodegradable and biocompatible polyester and a hydrophobic semicrystalline synthetic polymer, which has been studied widely for tissue regeneration and wound-healing applications as it encourages rapid healing with a low inflammatory response. The reason for its usage in various biomedical application is its exceptional blend capability, superior rheological behavior, and viscoelastic properties. PCL can be easily adapted by various fabrication techniques and is a Food and Drug Administration approved polymer with european commission (CE) mark registration. However, the major factor that limits the use of PCL in biomedical applications is its hydrophobicity. Previous studies from our group have proven that the blending of herbal AV extract with Poly(l-lactic acid)-co-poly (ε-caprolactone) (PLACL) has improved the hydrophilicity and provided better cell proliferation.[18] Hence, in this study, we decided to explore and investigate the effect of AV-doped PCL matrixes in an *in vivo* environment for healing chronic wounds. The performance of the developed mat was tested under *in vivo* conditions with a rat model.

EXPERIMENTAL

Materials

PCL (weight-average molecular weight = 70,000–90,000) was procured from Sigma-Aldrich (India). AV powder was procured from a locally available herbal medicine shop at Adyar Chennai. Chloroform and methanol of medical grade were purchased from SRL India and used as received.

Preparation of the Concentrated AV Extract

AV powder was dissolved in various concentrations (5, 10, and 15%) in a chloroform–methanol mixture (6 : 4). AV powder was refluxed for 6 h at 60°C, and the insoluble components were filtered with Whatmann No. 1 filter paper.[21,22] To remove the suspended materials and attain a clear homogeneous solution, the extracted solution was filtered through a membrane filter (pore size = 0.25 μm) with a sintered crucible and suction pump, and the residue was discarded. The obtained AV extract solution was used throughout the study.

Preparation of the Electrospinning Solutions

The PCL–AV solution for electrospinning was prepared with the concentrated chloroform–methanol extract of AV with various concentrations (5, 10, and 15%). In brief, 8% w/v PCL was prepared with the extract solution as a solvent. The solution was then transferred to a 5-mL syringe with a blunt-ended needle (18-mm gauge). The syringe was mounted on a horizontal electrospinning setup. A high-voltage supply of 17 kV was connected to the needle of a syringe pump (KD Scientific), and the generated nanofibers were collected on a grounded aluminum plate. The distance between the collector and the needle was maintained at 12 cm throughout the experiment with a flow rate of 1 mL/h. Almost 7 mL of electrospinning solution was electrospun to obtain a scaffold that was 0.25 mm thick for the animal wound-healing study. The surface morphology of the specimens was characterized with a scanning electron microscope (Hitachi S-3400) after the gold sputtering of the specimens. The specimens were gold-sputtered to attain a better quality image by means of charge dissipation and the improvement of the secondary electron signal. Fourier transform infrared (FTIR) spectroscopic analysis of the pure PCL and AV-extract-incorporated electrospun scaffolds was performed on a Bruker Optik Gmbh Tensor 27 FTIR system spectrophotometer (Germany) over the range 500–4000 cm^{-1} at 16 scans/min.

Water Contact Angle

Static wettability of the nanofiber matrixes were studied with the contact angle measurement method with water drops. A drop of purified water was placed on to the surface of the mats with a microsyringe attached to the goniometer. Images were captured by a high-resolution camera attached to the analyzer, and the contact angles were measured with the drop shape analysis method (Easy Drop, Kruss, Germany). At least four replicates were carried out to obtain a concordant result.

Degree of Swelling

The percentage swelling or the water-absorbing capacity of the nanofibers with and without AV was measured in a phosphate buffer solution of pH 7 solution at a temperature of 25°C for 24 h with four replicas. The excess solution adhered on the ultrafine mat was wiped with filter paper and weighed. The difference in weights was calculated with the following formula:

$$\text{Swelling}(\%) = \frac{W_s - W_d}{W_s}$$

where W_s is the weight of each sample after submersion in the buffer saline and W_d is the weight of the sample before submersion in the buffer saline.

Water Vapor Permeability

The water vapor permeability of developed herbal scaffolds was determined through the evaluation of the water vapor transmission rate (WVTR) through the membranes with ASTM standard E 96. Scaffolds cut into a predetermined size with a 35-mm diameter and a 0.25-mm thickness were used for the study. Nanofibrous scaffolds were mounted onto the plastic cup mouth; the cup was filled with water about three-quarters of its total volume without any penetration of water. The scaffolds were tightly fixed by means of paraffin tape along the periphery of the cups to prevent water loss across the boundary. The whole setup was maintained at 37°C with a 35% relative humidity in an environmental chamber. At regular intervals, the samples were weighed, and the weight loss was determined. A graph was plotted as the weight loss versus time

and from the graph slope, we calculated WVTR from the following formula:

$$\mathrm{WVTR} = \frac{\mathrm{Slope} \times 24}{A}\left[(\mathrm{g/m^2/day})\right]$$

where A is the area of the scaffolds (m^2). Four sets of samples were maintained to obtain the replicable results.

In Vitro Blood Compatibility Assay

To investigate the hemolytic activity of the scaffolds, human blood was collected in a sterile test tube containing 3.8% sodium citrate in the ratio 9 : 1 (blood–anticoagulant). The scaffolds with and without AV extract were UV-sterilized for 30 min and stabilized with 1 mL of saline for 24 h in sterile centrifuge tubes at 37°C in an incubator. Saline was subsequently removed from the tubes after 24 h, and a total volume of 0.625 mL of blood was added and incubated for 20 min at room temperature. After the incubation, 5 mL of freshly prepared saline was added to stop hemolysis and incubated for 1 h at room temperature. The sample was centrifuged at 750 G for 10 min. A blood sample with deionized water served as a positive control, and sterile saline served as a negative control. The supernatants were collected from each tube and read at 545 nm with an UV spectrophotometer. From the absorbance values obtained, the percentage hemolysis was calculated with the following formula:

$$\mathrm{Hemolysis}(\%) = \frac{\mathrm{OD\ for\ the\ test\ sample} - \mathrm{OD\ for\ the\ negative\ control}}{\mathrm{OD\ for\ the\ positive\ control} - \mathrm{OD\ for\ the\ negative\ control}}$$

where OD is the Optical Density.

Animal Wound-Healing Model

Eight-week-old female Wistar rats weighing 200–250 g were used for this study. All animals were maintained under constant ambient conditions (temperature = 25 ± 1°C) and given access to a standard diet and drinking water. PCL mats and PCL–AV (15%)-incorporated nanofiber scaffolds were used for the *in vivo* study. All of the animal experimental procedures were carried out in accordance with the Kovai Medical Centre and Hospital (KMCH) College of Pharmacy, Coimbatore, India, guidelines with ethical approval number KMCERT/PhD/05/2013–2014. Before the experiments were conducted, all of the scaffolds were sterilized under UV for 1 h. Animals were divided into four groups with six animals in a group: open wound (group I), Vaseline gauze (group II), PCL control (group III), and PCL–AV (group IV) blend (15% AV). The animals were anesthetized with ketamine (40 mg/kg). Anesthetized animals were clamped, and the hairs on the back of the rats were removed with shaver and depilatory cream. A full thickness of incision (1.5 × 1.5 cm^2) was made on the shaved region of the rats with a wound-excision method. The wounded area was cleaned with a povidone–iodine solution and wiped with distilled water with cotton. The wounds were then covered with specified dressings topically on regular basis on the wound bed from day 0 to day 19 to study the wound-healing properties. After wounding, the animals were housed in individual cages to monitor distress and other complications. On prespecified days, the rats were euthanized, and the tissues were dissected for staining assay.

Wound Closure Analysis

We measured the percentage wound closure every day from 1 to 14 days by copying the wound with transparent sheets and calculating the area of the wounds. The wound closure rate was calculated with the following formula:

$$\mathrm{Wound\ closure\ rate}(\%) = \frac{\mathrm{Area\ of\ wound\ on\ day\ 0} - \mathrm{Area\ of\ wound\ on\ day}\ n}{\mathrm{Area\ of\ wound\ on\ day\ 0}} \times 100$$

Histological Analysis

The wound specimens on specified days were stained with hematoxylin and eosin staining to observe the epithelialization and granulation of the reconstituted tissues. The covered nanofiber membranes were removed from wound areas, and the healed wound tissues were dissected from the rats under anesthesia. Harvested skin tissues were fixed with 4% paraformaldehyde, processed with a microtome, stained and viewed under light microscope embedded in paraffin. The examined tissues were photographed and analyzed for their tissue morphology.

RESULTS AND DISCUSSION

Water Contact Angle and Water Vapor Permeability

Wounds are injuries that result in a disruption of the skin surface. Wound healing is dependent on numerous factors, in which moisture plays a key role. Wound healing involves the migration of the cells from the wound edges to close the wound, and in a dry environment, cell migration is restricted. Additionally, a moist wound maintains optimal wound temperature and reduces the rate of infection and scaring. Hence, the developed wound dressing should provide an ambience that aids in wound healing. The developed nonwoven membranes were evaluated with a contact angle tester to assess their wettability. If the contact angle is lower, the material is more prone to be more hydrophilic. In this study, PCL, a biocompatible polyester polymer, was selected to prepare wound dressings. The PCL polymer possesses the good structural integrity required for a wound dressing but it lacks wettability. The polymer is highly hydrophobic; this is evident from the observed high contact angle of 125°. AV, a herbal drug, has been used from time immemorial for wound-healing applications. However, the coupling of a drug with wound dressings is generally carried out topically. To overcome the hydrophobicity of PCL and to achieve better wound-healing, AV was incorporated at concentrations of 5, 10, and 15% in the polymer matrixes. The incorporation of AV extract led to a drastic decrease in the contact angles. Contact angles of 67, 42, and 22° for 5, 10, and 15% AV-doped samples were observed (Figure 1). The increased hydrophilicity was attributed to the presence of water-absorbing groups in AV. As expected, an increase in the AV concentration resulted in an increased hydrophilicity in the mats. This result suggests that the developed wound-dressing material could be used for skin tissue engineering applications. Moreover, good moisture balance needs to be achieved as the water loss from the wound should be at an optimal rate, as reported in

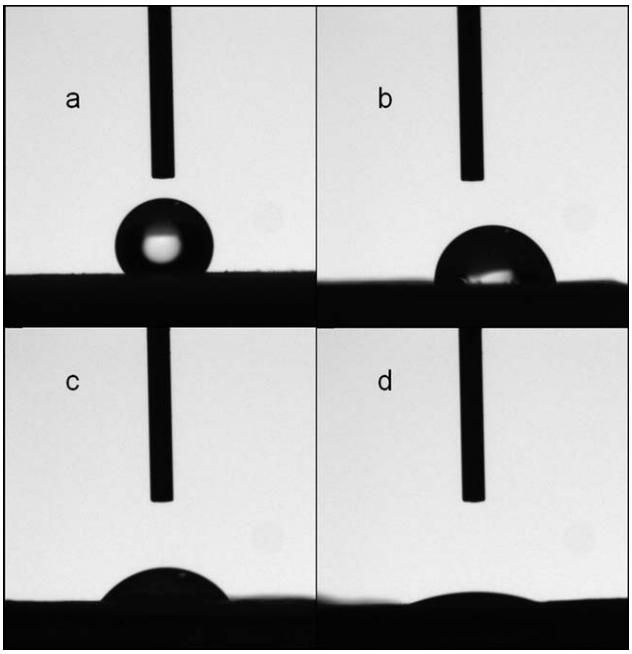

Figure 1. Nanofiber matrixes showing water contact angles: (a) PCL, (b) 5% AV, (c) 10% AV, and (d) 15% AV.

literature.[5] It has been well documented in the literature that the evaporative water loss for normal skin is about 204 g m^{-2} day^{-1} and that for injured skin can range from 279 to 5130 g m^{-2} day^{-1}.[5] As expected, the WVTR values of the developed dressings were found to be in the specified range; for PCL, it was lower, and for the AV-incorporated wound dressings, it was higher, about 2724 g m^{-2} day^{-1} (Figure 2 and Table I).

Surface Characterization and FTIR Studies

The scanning electron microscopy images of the pristine PCL sample and AV-doped samples are shown in Figure 3. The average diameters of the pristine PCL were in the range

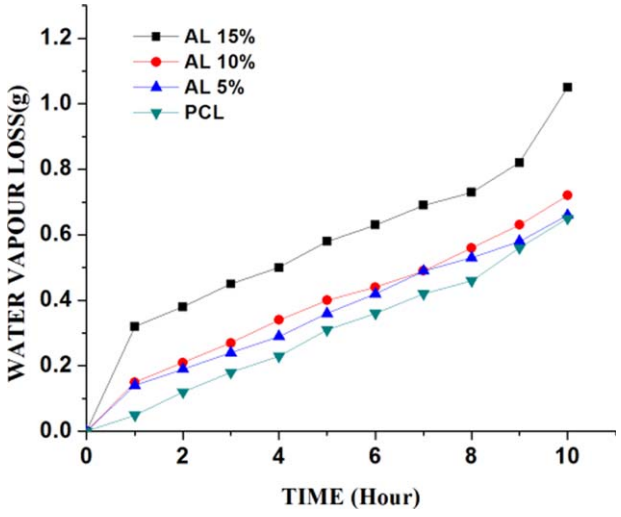

Figure 2. Water vapor loss for PCL and AV-incorporated nanofiber matrixes. [Color figure can be viewed in the online issue, which is available at wileyonlinelibrary.com.]

Table I. WVTR Values for the PCL–AV Dressings

Sample number	Sample	Water vapor evaporation rate (g m^{-2} day^{-1})
1	Control	2729
2	PCL	1623
3	PCL-AV 5	1801
4	PCL-AV 10	1933
5	PCL-AV 15	2724

192 ± 65 nm, and those of the AV-doped fibers were in the range 247 ± 77, 346 ± 20, and 460 ± 50 nm for 5, 10, and 15%, respectively. With increasing concentration of AV in the polymer, there was an increase in the diameter of the fibers. The FTIR spectrum of PCL and its blends with AV extract are presented in Figure 4. The FTIR spectrum of PCL shows its characteristic frequency vibrations. From the figure, we determined that the symmetric and asymmetric stretching vibrations of the CH_2 groups present in PCL occurred at 2870 and 2945 cm^{-1}. The C═O stretching vibrations of the ester group appear with an intense sharp peak at 1728 cm^{-1}, and the CH_2 bending vibration peaks occurred at 1362 and 1465 cm^{-1}. The —C—OO vibrations gave its characteristic peaks at 1291, 1238, and 1181 cm^{-1}. The —C—O—C symmetric and asymmetric stretching vibrations were also seen at 1047 and 1009 cm^{-1}, and its corresponding vibrations were seen at 961 cm^{-1}. The peak at 729 cm^{-1} was due to the CH_2 rock, whereas the characteristic peak of the PCL–AV blend showed the combined peaks for the virgin PCL and AV, respectively. The absorption bands at 1578 and 1736 cm^{-1} were assigned to the C═O of PCL and *O*-acetyl esters of AV. Furthermore, a typical peak in the spectral region of 1645 cm^{-1} may have been due to the carboxyl asymmetric stretching and O—H deformation. The aromatic vibrations of compounds present in the AV extract were also observed at 1600, 1500, and 1450 cm^{-1}, and these confirmed their presence and the better incorporation of AV with PCL.

Degree of Swelling

Wound-dressing materials are required to possess good water uptake and good water vapor permeability to maintain a proper moisture balance at the infected site. The water uptake and permeation particularly depend on the type of polymer and materials. In a wound environment, the exudates and other fluids coming out of the wound need to be absorbed to hasten the healing process. The rate of absorption of the exudates and retention are significant factors in the quick healing of necrotic tissues in the wound. Moreover, the autolytic debridement of the wounds is promoted by quick absorption. The study of the percentage water uptake of the mat will give an idea of the ability of a mat to absorb fluids. The percentage water uptake depends on the swelling characteristics of the mat and the degree of hydrophilicity. The percentage water uptake of the PCL and PCL–AV-incorporated mats are given in Figure 5. The water uptake increased with increasing AV composition in the blend, and this, thereby, implied that the mat became

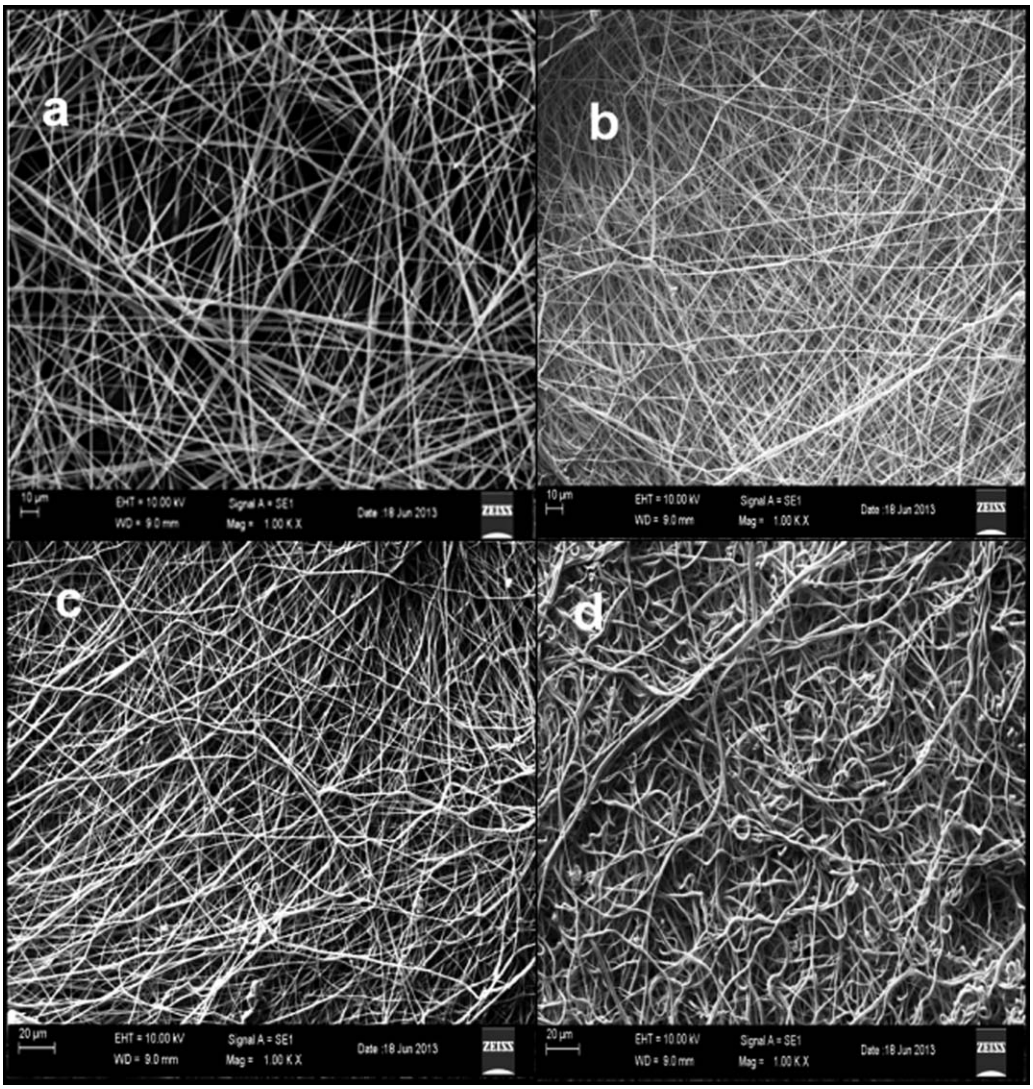

Figure 3. Scanning electron micrographs of electrospun matrixes showing (a) PCL, (b) 5% AV, (c) 10% AV, and (d) 15% AV.

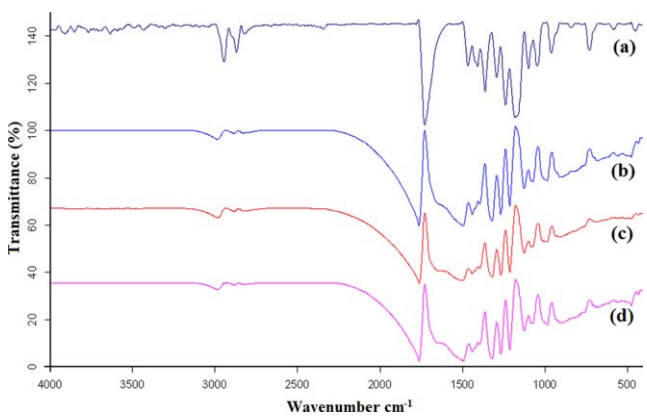

Figure 4. FTIR spectra of the PCL and AV-doped nanofibrous matrixes. [Color figure can be viewed in the online issue, which is available at wileyonlinelibrary.com.]

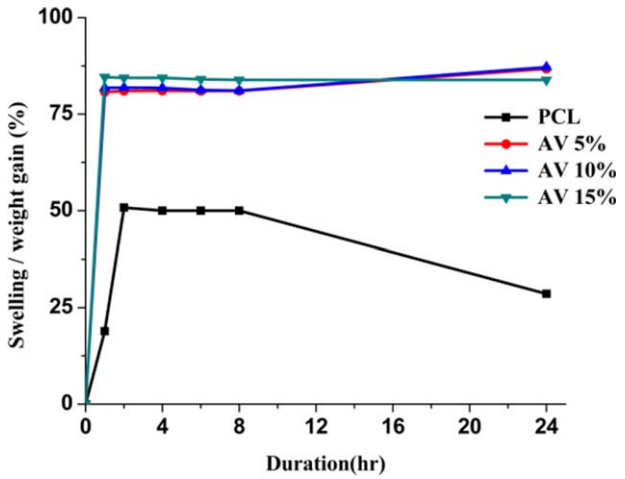

Figure 5. Swelling/water absorption capacity of the PCL and AV-incorporated samples. [Color figure can be viewed in the online issue, which is available at wileyonlinelibrary.com.]

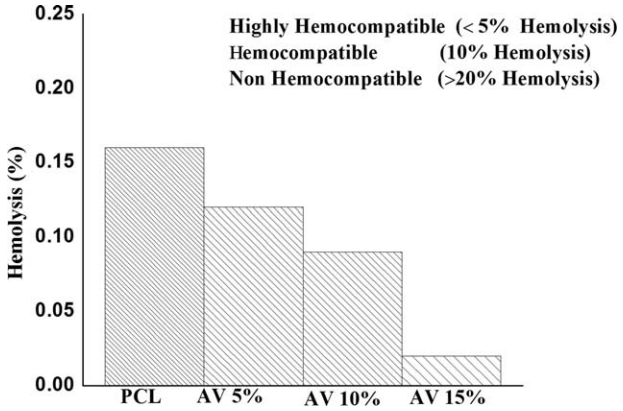

Figure 6. Blood compatibility behavior of the PCL and AV-incorporated nanofiber dressings.

hydrophilic with the incorporation of the AV extract. Moreover, it was also observed in the figure that the blended mats absorbed and retained water consistently throughout the period of study; this indicated that it could be an ideal dressing material for chronic or occlusive wounds.

The PCL matrixes showed a water-absorbing capacity of 20% for 1 h, whereas in all the AV-incorporated samples, the water-absorbing capacity increased from 75 to 80% with respect to the concentration of AV incorporation. In a biological environment, biomolecules such as enzymes, proteins, and other macromolecules function with respect to the hydrophilic properties of the membranes with respect to swelling to absorb the molecules that enhance wound healing. Moreover, after 24 h of immersion, the water retention of PCL decreased from 50%, but the AV-incorporated samples exhibited no change in this property.

Blood Compatibility: Hemolysis

Hemocompatibility is a basic requirement of a biomaterial to be implanted or tested for any material that will come into contact with blood to determine the safety parameters of the material in the human body. Incompatible biomaterials in contact with blood may induce erythrocyte lysis, particularly during prolonged contact with the cell surface, and will cause adverse effects of tissue rejection. The lysis of red blood cells and the release of hemoglobin and its cellular constituents may trigger hemolytic anemia, neutropenia, and thrombocytopenia to the host tissues. The developed materials were assessed with hemolytic assay to study the compatibility of the PCL and PCL–AV-incorporated membranes. The effect of the integrity of the PCL and PCL–AV loaded membrane with red blood cells was studied. However, PCL and PCL–AV extract loaded membranes did not exhibit any red blood cell rupture but showed that the membranes were highly compatible. The percentage hemolysis of the PCL and AV-loaded membranes (5, 10, and 15%) were calculated and found to be within normal limits, as shown in Figure 6, and it was also explicit that an increase in the AV concentration had no adverse effect on hemolysis. Moreover, the results suggest that the produced membranes were biologically compatible and were suitable materials for tissue engineering applications.

In Vivo Wound-Healing Model

The wound-healing efficiency of the developed nanofiber was studied with a rat model. The pure PCL nanofibers and PCL mat loaded with 15% AV extract were investigated with a rat wound-healing model. Wounds created on the backs of the rats were examined for a period of 19 days postwounding. The wounds were covered with PCL, PCL–15% AV, nothing (open wound), and Vaseline gauze, respectively. As shown in Figure 6, the wounds covered with AV-extract-incorporated nanofibers healed faster than the PCL and bare wound in comparison with the Vaseline gauze covered wounds. After 5 days postwounding, no infection was observed on the PCL–AV covered wounds, whereas in bare wounds, infection was observed, and the wounds were inflamed with pus formation on the surface. During the postwounding period, no adverse reactions, such as edema or swelling, skin irritation, or infection, were found at the wound site with AV-extract-incorporated nanofibers. This was attributed to the presence of active compounds present in the nanofiber dressings, which were found to be highly biocompatible.

Wound Closure Analysis

The examination of the wound area contraction after a defined interval from postwounding was calculated. Figure 7 shows the photographs of a wound from day 0 to day 19 postwounding. On day 5, in all of the groups, no significant reduction was observed, whereas on day 7, the wounds started healing well in a comparable manner for group IV (test). This showed a contraction of 33% for group III, a contraction of 33% for group I, and a contraction of 32% for group II. On day 14, the wound percentage contraction increased significantly for group IV to about 78% compared with the open wound, which had a contraction of about 70%. However, by day 19, the overall healing was good in all of the groups, but complete healing was observed only in group IV with the AV-extract-incorporated dressings, which showed a contraction in the wound area of 97%. The reduction in the wound area revealed that the AV-extract-incorporated dressing efficiently healed the wound without any cytotoxic effects and was biologically active in the wound environment to provide moist healing.

Histological Evaluations

In wound healing, the complex and dynamic process of tissue regeneration is divided into four distinct phases: (1) homeostasis, (2) inflammation, (3) proliferation or granulation, and (4) maturation or remodeling. A healing cascade persists to continue from the time of injury to the day of complete healing; it lasts for almost 21 days, depending on the injury. During healing, the wounds contract toward the edges, with the formation of granulation tissues and epithelialization of wound tissues. Inflammatory granulation tissues were found on the epidermal layer of the wounded tissue after hemostasis and could be evaluated by the staining of the dissected tissues of the wounded rats.

Histological evaluation of this study was obtained for the 5th, 9th, and 11th days to evaluate the formation of re-epithelialized tissue. Figure 8 shows the histology results for the all four groups of animal studied on the 5th, 7th, and 11th days postwounding. The result on day 5 suggested that the group I bare wounds

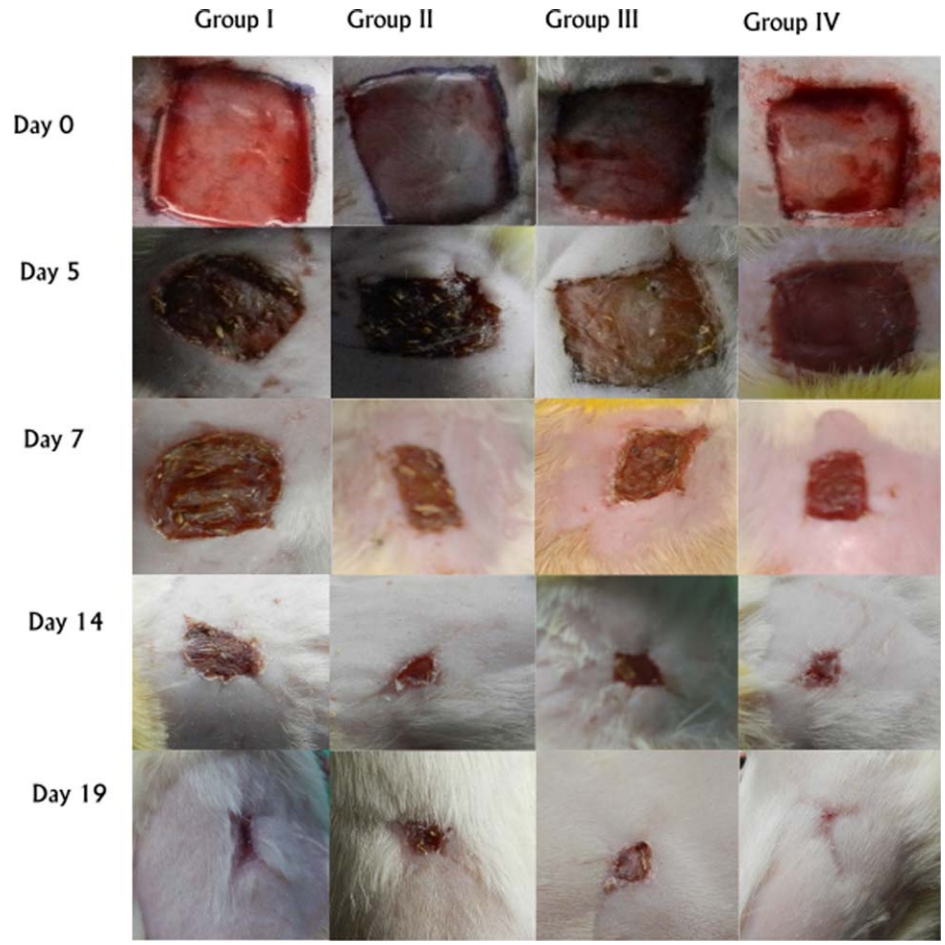

Figure 7. Images showing the closure of wounds on various days for the PCL and AV-incorporated nanofiber dressings. [Color figure can be viewed in the online issue, which is available at wileyonlinelibrary.com.]

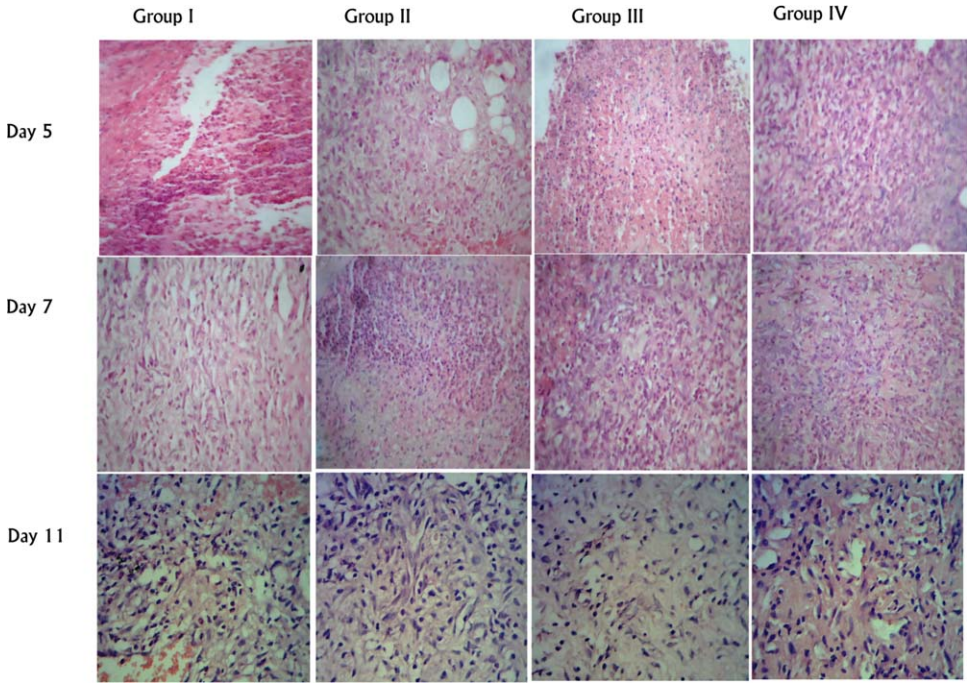

Figure 8. Histology of the excised wounds with hematoxylin and eosin staining. [Color figure can be viewed in the online issue, which is available at wileyonlinelibrary.com.]

showed a significant number of inflammatory cells with polymorphs and no formation of granulation tissue or fibroblast was observed, whereas in group IV, the AV-incorporated sample group, granulation tissue composed of fibroblast and vascular proliferation was observed. Groups II and III showed fibroblast proliferation, mild inflammation, and no epithelial proliferation. On day 7, the bare wound showed dense acute inflammation, areas of hemorrhaging, and no vascular proliferation. In the AV-incorporated dressings, evidence of fibrosis, the formation of capillaries, and collagen fibers on the granulation tissue with epidermal layers was visible. The histology results of day 11 revealed faster healing with older granulation tissue and an unremarkable epidermal layer. In the control and other groups, less formation of fibrin exudates with granulation and a remarkable epidermis were observed. From the histological observations, it was evident that the *in vivo* experiment carried out with the AV-extract-incorporated nanofiber membranes showed a significant rate of healing compared to the other groups. After the 11th day of observation, this wound began to heal more rapidly than the PCL and open wound, with a gradual increase in tissue formation and the contraction of the wound without any infection. In the control groups, inflammation and infection was observed, and healing was delayed compared to the herbal-extract-incorporated dressings. From the literature, it is known that keratinocyte cells can easily migrate toward the outer wound layer over a moist environment to form the scab, and epidermal cells can migrate two times faster in a moist wound than in a dry wound. The nanofibers incorporated with AV extract offered an enhanced hydrophilic environment to the wound and, thereby, facilitating the wound to heal rapidly. Moreover, the prime reason of group IV to heal quickly compared to the other groups may have been the presence of active ingredients of AV for collagen secretion and the support provided by the nanofiber membranes to the cells for better adherence, nutrient supply, and protection against infectious pathogens.

CONCLUSIONS

AV-incorporated dermal wound-dressing nanofibrous matrixes were developed. The incorporation of AV in the matrixes led to an increased hydrophilicity and an increase in the degree of swelling and water vapor permeability. The AV-incorporated matrixes also exhibited good water retention properties, even after 24 h. The hemolytic studies confirmed that the developed matrixes were biocompatible. *In vivo* studies in a rat model further confirmed that the developed matrixes aided in quicker healing compared to the bare wound and PCL matrixes.

REFERENCES

1. Zahedi, P.; Rezaeian, I.; Ranaei Siadat, S.; Jafari, S. H.; Supaphol, P. *Polym. Adv. Technol.* **2010**, *21*, 77.
2. Zahedi, P.; Rezaeian, I.; Jafari, S. H. *J. Mater. Sci.* **2013**, *48*, 3147.
3. Raveendran, R.; Bhuvaneshwar, G. S.; Sharma, C. P. *J. Biomater. Appl.* **2013**, *27*, 7,811.
4. Balakrishnan, B.; Mohanty, M.; Umashankar, P. R.; Jayakrishnan, A. *Biomaterials* **2005**, *26*, 6335.
5. Xu, H.; Ma, L.; Gao, C.; Han, C. *Polym. Adv. Technol.* **2007**, *18*, 869.
6. Choi, J. S.; Leong, K. W.; Yoo, H. S. *Biomaterials* **2008**, *29*, 587.
7. Kumar, B.; Vijayakumar, M.; Govindarajan, R.; Pushpandagan, P. *J. Ethnopharmacol.* **2007**, *114*, 103.
8. Kondo, T.; Ishida, Y. *Forensic Sci. Int.* **2010**, 203, *93*.
9. Peng, L. H.; Chen, X.; Chen, L.; Li, N.; Liang, W. Q.; Gao, J. Q. *Biol. Pharm. Bull.* **2012**, *35*, 881.
10. Gomes, S.; Llamas, J. G.; Leonor, I. B.; Mano, J. F.; Reis, R. L.; Kaplan, D. L. *Macromol. Biosci.* **2013**, *13*, 444.
11. Payam, Z.; Iraj, R.; Seyed, H. J. *J. Mater. Sci.* **2013**, *48*, 3147.
12. Sudheesh Kumar, P. T.; Vinoth-Kumar, L.; Anilkumar, T. V.; Ramya, C.; Reshmi, P.; Unnikrishnan, A. G.; Shantikumar, V. N.; Jayakumar, R. *Appl. Mater. Interfaces* **2012**, *4*, 2618.
13. Alok, M.; Versha, P.; Geeta, P.; Ishan, D.; Deepak, K. *Int. J. Res. Phytochem. Pharmacol.* **2011**, *1*, 207.
14. Sadegh, K. A.; Mohammad, H. A.; Zohreh, H.; Niloofar, B. F. *Carbohydr. Polym.* **2012**, *87*, 2058.
15. Ravi, S.; Kabilar, P.; Velmurugan, P.; Ashok Kumar, R.; Gayathri, M. *J. Exp. Sci.* **2011**, *2*, 10.
16. Ibrahim, U.; Selda, K.; Ali, G.; Tutku Caren, K.; Mehmet Levent, A. *J. Biol. Chem.* **2010**, *38*, 19.
17. Suganya, S.; Venugopal, J.; Ramakrishna, S.; Lakshmi, B. S.; Giri Dev, V. R. *J. Appl. Polym. Sci.* **2014**, *131*, 39835.
18. Suganya, S.; Venugopal, J.; Agnes Mary, S.; Ramakrishna, S.; Lakshmi, B. S.; Giri Dev, V. R. *Iran. Polym. J.* **2014**, *23*, 237.
19. Sabitha, M.; Sanoj, R. N.; Amrita, N.; Vinoth-Kumar, L.; Shantikumar, V. N.; Jayakumar, R. *Nanoscale* **2012**, *4*, 239.
20. Pandarinathan, C.; Sajithlal, G. B.; Gowri, C. *Mol. Cell. Biochem.* **1998**, *181*, 71.
21. Chellamani, K. P.; Vignesh Balaji, R. S.; Veerasubramanian, D.; Sudharsan, J. *J. Acad. Indus. Res.* **2014**, *2*, 622.
22. Agnes Mary, S.; Giri Dev, V. R. *J. Text. Inst.* **2014**, DOI: 10.1080/00405000.2014.951247